2016 IEEE International Conference on Robotics and Automation (ICRA)
Stockholm, Sweden, May 16-21, 2016

Model Predictive Control for Dynamic Footstep Adjustment Using the Divergent Component of Motion

Robert J. Griffin and Alexander Leonessa*

***Abstract*— This paper presents an extension of previous model predictive control (MPC) schemes to the stabilization of the time-varying divergent component of motion (DCM). To address the control authority limitations caused by fixed footholds, the step positions and rotations are treated as control inputs, allowing the generation and execution of stable walking motions, both at high speeds and in the face of disturbances. Rotation approximations are handled by applying a mixed-integer program, which, when combined with the use of the time-varying DCM to account for the effects of height changes, improve the versatility of MPC. Simulation results of fast walking and step recovery with the ESCHER humanoid demonstrate the effectiveness of this approach.**

I. Introduction

Although there has been much improvement in humanoid walking performance, significant progress is still needed for bipeds to rival the mobility of humans. A critical component for performance in realistic environments is the ability to compensate for surface uncertainties and disturbances. The control authority afforded by a fixed footstep plan for stabilizing the center of mass (CoM) is limited, though, as the center of pressure (CoP) must remain within the base of support to satisfy no-tipping conditions. The step positions found by many high level footstep planners do not account for the CoM dynamics when generating plans, and rely on heuristically tuned weights to generate feasible footholds [1–3]. One method to account for these exogenous inputs is to allow adjustment of the desired step position based on the current CoM state.

A common approach for CoM trajectory planning is to find acceptable CoP trajectories and then use the linear inverted pendulum (LIP) dynamics [4–7], noting the equivalency of the CoP and zero-moment point in x and y [8]. In [9], Pratt split the CoM dynamics into stable and unstable parts by defining the capture point (CP) as the location above which the CoM will stop. The CP was then extended to its 3D equivalent, the divergent component of motion (DCM) [10] and time-varying DCM [11], enabling planning and tracking in three-dimensions. Feedback control of only the unstable component of the CoM dynamics has been shown to be an effective method for stabilizing walking motions [10–15]. To recover from large disturbances, humans often adjust their footsteps to increase their base of support. Most step adjustment feedback methods, however, involve some sort of heuristic [10, 15], rather than dynamics-based solution.

The authors are with the Terrestrial Robotics, Engineering & Controls (TREC) Laboratory at Virginia Tech. (e-mail: robert.griffin@vt.edu)

*This material is based upon work supported by (while serving at) the National Science Foundation.

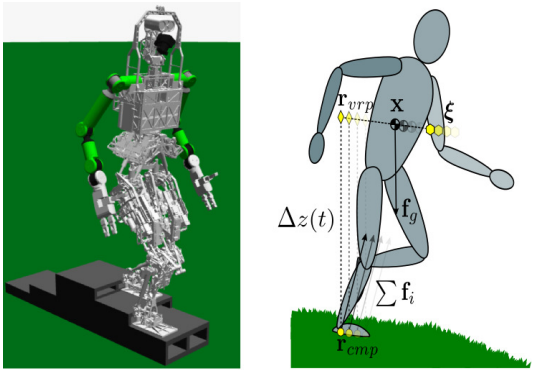

Fig. 1. Left: ESCHER walking on uneven terrain in simulation. Right: DCM dynamics and external forces acting on an articulated humanoid.

An alternative to tracking preplanned CoM trajectories with feedback controllers is online model predictive control (MPC) schemes that calculate control inputs using the current state. Preview control has been used to plan feasible CoP trajectories [5, 16], with the structure being relaxed in [17, 18] by treating the step positions as control inputs, allowing successful rejection of disturbances to step adjustment. MPC has also been extended to the unstable CP dynamics using only the CoP as the control input [19].

While MPC schemes have been quite successful, they often do not have the same versatility as feedback control methods. The effects of changes in CoM height over uneven terrain are typically not considered in CoP based methods, with notable exceptions in [20–22]. To account for these effects, the authors propose a novel formulation of the MPC problem using the time-varying DCM dynamics [11]. This will be done in such a way as to treat the step positions as control inputs. The formulation will also allow consideration of step rotations as control inputs, a currently unaddressed issue due to its nonlinear nature. Rotation is a crucial component as it determines the reachable set, affecting CoM motion over the course of the step plan. As both height and heading changes are essential to navigating environments outside the lab, these shortcomings limit the current use of real-time MPC methods in fielded robotics.

This paper is organized as follows: Section II reviews the time-varying DCM formulation. Section III reviews the trajectory planning and execution presented in [11]. The proposed MPC formulation is presented in Section IV, proposing methods for the treatment of step positions and rotations as control inputs. Section V presents simulation results of the 38-DoF model of the ESCHER humanoid, demonstrating the capabilities of the proposed MPC scheme.

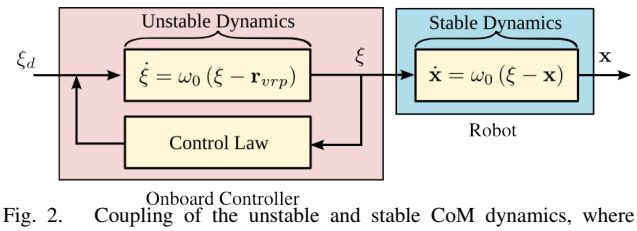

Fig. 2. Coupling of the unstable and stable CoM dynamics, where ξ represents the DCM position and $\mathbf{x}$ the CoM position.

II. Control of Center of Mass Dynamics

The problem of bipedal balancing can be analyzed using CoM models and their relation to ground reaction forces. The following gives a brief background of these models, from the classical linear inverted pendulum (LIP) model to the more recent time-varying divergent component of motion (DCM).

A. Linear Inverted Pendulum Model

The LIP model has been widely used for biped walking [4–7], as it allows the centroidal dynamics of the robot to be linear and decoupled in x and y. The dynamic equations for the horizontal acceleration of the CoM in the LIP are given by

$$\ddot{x}_{com} = \omega_0^2 (x_{com} - p_x), \quad \ddot{y}_{com} = \omega_0^2 (y_{com} - p_y), \quad (1)$$

where $\mathbf{x} = [x_{com}, y_{com}, z_{com}]^T$ is the CoM position, $\omega_0 = \sqrt{\frac{g}{\Delta z_{com}}}$ is the natural frequency, and $\mathbf{p} = [p_x, p_y, p_z]^T$ is the location of the torque-free pendulum base joint. This point is equivalent to the CoP, meaning the ground reaction force is colinear with the vector $(\mathbf{x} - \mathbf{p})$. CoM trajectories can then be found from feasible CoP trajectories, and executed using either feedback or MPC strategies on both position and force controlled robots.

B. Time-Varying DCM Definition

An alternate description of the CoM state is to transform it into stable and unstable first order components, as shown in Fig.2. The unstable part is called either the capture point (CP) [9] (the two dimensional point above which the CoM will stop) or the DCM [10] (the three dimensional point at which the CoM will come to rest). First introduced in [11], the time-varying DCM, shown in Fig.1, allows the natural frequency of the LIP, ω_0, to vary with time, and is defined as

$$\boldsymbol{\xi} = \mathbf{x} + \frac{1}{\omega(t)} \dot{\mathbf{x}}. \quad (2)$$

This relaxation allows the height of the LIP to vary with changes in uneven terrain, resulting in improved control of the vertical CoM motion during locomotion. The unstable time-varying DCM dynamics are then given by

$$\dot{\boldsymbol{\xi}} = \left(\omega - \frac{\dot{\omega}}{\omega} \right) (\boldsymbol{\xi} - \mathbf{r}_{vrp}), \quad (3)$$

where $\mathbf{r}_{vrp}$ is the time-varying virtual repellent point (VRP) [11]. The time-varying VRP is defined in terms of the time-varying enhanced centroidal moment pivot (eCMP) [11] as

$$\mathbf{r}_{vrp} = \mathbf{r}_{ecmp} + \frac{\mathbf{g}}{\omega^2 - \dot{\omega}}, \quad (4)$$

where $\mathbf{g} = [0, 0, g]^T$ and

$$\mathbf{r}_{ecmp} = \mathbf{x} - \frac{\sum \mathbf{f}_c}{m (\omega^2 - \dot{\omega})}, \quad (5)$$

where $\sum \mathbf{f}_c \in \mathbb{R}^3$ are the contact forces acting on the CoM. Given the VRP setpoint and CoM estimate, the desired linear momentum rate of change, $\dot{\mathbf{l}}_d$, can be found using

$$\dot{\mathbf{l}}_d = m \left(\omega^2 - \dot{\omega} \right) (\mathbf{x} - \mathbf{r}_{vrp}).$$

From Eq. (2), the stable first-order CoM dynamics are

$$\dot{\mathbf{x}} = \omega (\boldsymbol{\xi} - \mathbf{x}), \quad (6)$$

showing that the CoM converges to the DCM with a time constant $\frac{1}{\omega_0}$.

III. Related Work

In [11], Hopkins et al. presented a framework for planning and executing time-varying DCM trajectories using reverse-time numerical integration and feedback control. An MPC scheme is then used to generate smooth DCM trajectories using DCM acceleration as the control input. This approach is outlined in the following section.

A. Planning and Tracking DCM Trajectories

The $\omega(t)$ trajectory can be computed through reverse-time integration of the nonlinear ω dynamics, given CoM height trajectories planned using the method outlined in [11]. Then, the VRP trajectory can be found from a desired CoP trajectory using Eq. (4). Note that, when planning CoM trajectories, angular momentum is typically held at zero, implying the collocation of the CoP and eCMP, making Eq. (4) $\mathbf{r}_{vrp} = \mathbf{r}_{cop} + \frac{\mathbf{g}}{\omega^2 - \dot{\omega}}$. This result can be used with the $\omega(t)$ trajectory to generate the DCM trajectory using Eq. (3).

Based on the definition of the DCM dynamics, the time-varying DCM is unstable with respect to the VRP. However, in reverse-time, the VRP acts as an attractor for the DCM,

$$\dot{\boldsymbol{\xi}}_r = -\left(\omega - \frac{\dot{\omega}}{\omega} \right) (\boldsymbol{\xi} - \mathbf{r}_{vrp}(t_r)), \quad \boldsymbol{\xi}(t_f) = \boldsymbol{\xi}_f, \quad (7)$$

where $\dot{\boldsymbol{\xi}}_r = -\dot{\boldsymbol{\xi}}$ is the reverse-time derivative of the DCM. The DCM trajectory can then be found through reverse-time integration, as well [11].

To track the DCM trajectory, the PI control law defined in [11], is used. While this controller has been demonstrated to work well on a variety of terrain [15], it does not allow the use of the desired step positions or rotations as control inputs, relying entirely on the achievable ground reaction forces from step positions found by a high level footstep planner for stabilization.

IV. DCM Model Predictive Controller

The MPC scheme in [11] can be generalized in a way similar to that presented in [17] to compute optimal DCM trajectories in x and y for a defined preview window using DCM accelerations as the control input. The DCM height trajectories can be planned and tracked using the approach

in [11], which is also used to find the final value for the preview window.

The DCM acceleration is chosen as a control input as it relates to minimizing the CoM jerk, resulting in smooth CoM trajectories. To allow for direction changes while walking, necessary for navigating real-world environments, rotation must also be considered. As such, the authors propose allowing the MPC scheme to decide the DCM acceleration, step positions in the x-y plane, and step rotation, making the control inputs $\mathbf{v}_u = \left[\mathbf{v}_{\ddot{\xi}}^T, \mathbf{v}_f^T\right]^T$, where $\mathbf{v}_{\ddot{\xi}} \in \mathbb{R}^{2N}$ is the discretized DCM acceleration vector in x and y of N timesteps, and $\mathbf{v}_f \in \mathbb{R}^{3m}$ is the vector of m foot positions and rotations, x, y and θ.

The following sections describe the formulation of the arguments for the MPC objective function, as well as the constraints on the step positions that allow consideration of step rotations.

A. DCM and VRP Recursive Dynamics

In order to compute the MPC arguments, the discrete-time DCM and VRP dynamics must first be defined. Due to the uncoupled nature of the DCM dynamics, the discretization is the same along both x and y axes, and is defined in [11]. The discrete-time DCM position and velocity trajectory, $\mathbf{v}_\xi \in \mathbb{R}^{2N}$, can be defined along a single axis as a function of linear operators $\mathbf{\Phi}_0^\xi \in \mathbb{R}^{2N\times 2}$ and $\mathbf{\Phi}_u^\xi \in \mathbb{R}^{2N\times N}$ by

$$\mathbf{v}_\xi = \mathbf{\Phi}_0^\xi \boldsymbol{\xi}_0 + \mathbf{\Phi}_u^\xi \mathbf{v}_{\ddot{\xi}}. \tag{8}$$

The discrete-time VRP trajectory, $\mathbf{v}_y \in \mathbb{R}^N$ can likewise be defined along a single axis as a function of linear operators $\mathbf{\Phi}_0^y \in \mathbb{R}^{N\times 2}$ and $\mathbf{\Phi}_u^y \in \mathbb{R}^{N\times N}$ by

$$\mathbf{v}_y = \mathbf{\Phi}_0^y \boldsymbol{\xi}_0 + \mathbf{\Phi}_u^y \mathbf{v}_{\ddot{\xi}}, \tag{9}$$

where $\boldsymbol{\xi}_0 \in \mathbb{R}^2$ is the initial DCM position and velocity [11].

B. DCM Reverse-Time Integration

As shown in Eq. (7), the VRP acts as an attractor in reverse-time, so stable trajectories can be found through reverse-time integration of the DCM. Numerical integration can be performed using Huen's method, leading to the discrete dynamics

$$\begin{aligned}\xi_{k-1} = &(D_{k-1} + (1 - \Delta t D_{k-1})\, D_k)\xi_k + \left(-\tfrac{1}{2} D_{k-1}\right) y_{k-1} \\ &+\left(-\tfrac{1}{2}\left(1 - \Delta t D_{k-1}\right)\right) y_k,\end{aligned} \tag{10}$$

where $D_k = \omega_k - \frac{\dot{\omega}_k}{\omega_k}$, and y_k is the VRP signal at time step k. The reverse-time integrated DCM signal can be calculated via linear operators that encode Eq. (10 by

$$\mathbf{v}_{\xi,s} = \mathbf{\Phi}_0^v \xi_f + \mathbf{\Phi}_u^v \mathbf{v}_{y,s}, \tag{11}$$

where $\mathbf{\Phi}_0^v \in \mathbb{R}^{N\times 1}$ and $\mathbf{\Phi}_u^v \in \mathbb{R}^{N\times N}$ in dimension, $\mathbf{v}_{y,s} \in \mathbb{R}^N$ is the discretized VRP input, and ξ_f is the desired final DCM position. Note that $\dot{\xi}_f$ is encoded in y_f.

The state equations (8) and (9) are functions of the current DCM state and control input. The new state equation (11), however, is a function of the final DCM objective and this VRP input. Some way of relating the VRP input to the control input is still needed.

C. Step Positions as Control Inputs

It can be seen from Eq. (4) that, in the x-y plane, $\mathbf{r}_{vrp} = \mathbf{r}_{ecmp}$, as $\mathbf{g} = [0,\ 0,\ g]^T$. Then, with the assumption that there is no desired angular momentum, the assumption that $\mathbf{r}_{vrp} = \mathbf{r}_{cop}$ is valid in x-y.

The CoP trajectory can be defined by a set of piecewise minimum-jerk trajectories, and can be found from the step positions using a series of linear operators. The operator $\mathbf{F}_e : \mathbb{R}^{m\times 2} \mapsto \mathbb{R}^{4\times 2}$, is defined to map the step positions in $\mathbf{v}_f$ to a vector of end conditions for each minimum-jerk segment. The operator $\mathbf{M} \in \mathbb{R}^{N\times 4} : \mathbb{R}^{4\times 2} \mapsto \mathbb{R}^{N\times 2}$ maps the vector of end conditions $\left(\mathbf{p}_0, \dot{\mathbf{p}}_0, \mathbf{p}_f, \dot{\mathbf{p}}_f\right)^T$ to the minimum-jerk trajectory of N discretized points. The reference VRP input along both axes, $\mathbf{v}_{y,s}$, in Eq. (10) is then defined as

$$\mathbf{v}_{y,s} = \mathbf{M}\left(\mathbf{P}_s + \mathbf{F}_e \mathbf{v}_f\right), \tag{19}$$

where $\mathbf{P}_s$ is a matrix consisting of initial CoP position and velocity and initial poses of both feet. Note that through this definition, $\mathbf{r}_{cop}$ is defined as going through the middle of the foot, offset by values in $\mathbf{P}_s$, guaranteeing no-tipping conditions are satisfied without the use of constraints.

Now that the DCM dynamics have been defined as functions of the initial state, final state, and control inputs, what remains is to formulate the objective function and constraints for the MPC.

D. Objective Function

The MPC scheme can be defined as a quadratic program (QP) with an objective function formulated by

$$\begin{aligned}\min_{\mathbf{v}_{\ddot{\xi}}, \mathbf{v}_f} \ &\tfrac{1}{2}\left(\mathbf{v}_\xi - \mathbf{v}_{\xi,s}\right)^T \mathbf{F}\left(\mathbf{v}_\xi - \mathbf{v}_{\xi,s}\right) + \tfrac{1}{2}\mathbf{v}_{\ddot{\xi}}^T \mathbf{R} \mathbf{v}_{\ddot{\xi}} \\ &+ \tfrac{1}{2}\left(\mathbf{v}_y - \mathbf{v}_{y,s}\right)^T \mathbf{Q}\left(\mathbf{v}_y - \mathbf{v}_{y,s}\right) + \tfrac{1}{2}\mathbf{v}_{\dot{\xi}}^T \mathbf{D} \mathbf{v}_{\dot{\xi}} \\ &+ \tfrac{1}{2}\left(\mathbf{v}_f - \mathbf{v}_{f,s}\right)^T \mathbf{T}\left(\mathbf{v}_f - \mathbf{v}_{f,s}\right),\end{aligned} \tag{20}$$

where $\mathbf{F}$, $\mathbf{Q}$, $\mathbf{T}$, $\mathbf{R}$, and $\mathbf{D}$ are the objective weighting matrices, described below. Separate weights for x and y can be specified in a desired frame, and transformed to the inertial frame via rotation matrices.

The weight $\mathbf{F}$ ensures the DCM acceleration tracks the reference signal $\mathbf{v}_{\xi,s}$ found from the step positions. In this implementation, a selection matrix, $\mathbf{S}_f \in \mathbb{R}^{1\times N}$, is applied to restrict tracking to the final value of the trajectory to eliminate discontinuities between the preview window and original trajectory. The weight $\mathbf{R}$ directly minimizes the DCM acceleration to produce smooth CoM motion. The next weight, $\mathbf{Q}$, defines the relationship between the DCM acceleration and the step positions. $\mathbf{T}$ ensures the step positions track those provided by the footstep planner. The final weight, $\mathbf{D}$, was introduced on implementation to damp the DCM trajectory by penalizing high frequency oscillations.

E. Reachability Constraints

In order to ensure that the step positions found by the MPC scheme are achievable, the positions must be constrained to be kinematically reachable by the robot. When considering a series of steps, this reachability region is strongly affected by the rotation of each step, ultimately determining the path

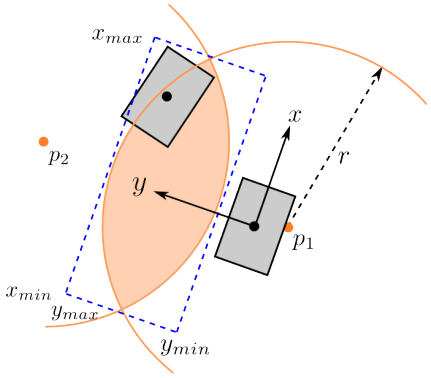

Fig. 3. The reachability set is described by two intersecting circles, shown by the shaded area, with limits shown by the dotted blue line.

the robot takes for the plan. As such, the rotation of the adjustment step is important to consider when formulating the reachability constraints.

First proposed in [1], the reachability set can be approximated by the intersecting region of two circles, as shown in Fig.3. The step position can be constrained to lie in the intersecting region through two convex quadratic constraints by requiring that, for each footstep, j,

$$\left\| \begin{bmatrix} x_j \\ y_j \end{bmatrix} - \left(\begin{bmatrix} x_{j-1} \\ y_{j-1} \end{bmatrix} + \begin{bmatrix} c_{j-1} & -s_{j-1} \\ s_{j-1} & c_{j-1} \end{bmatrix} \mathbf{p}_i \right) \right\| \leq r, \quad (21)$$

where s_j and c_j are introduced for each step to approximate $\sin\theta_j$ and $\cos\theta_j$ to ensure that the constraint remains convex and linear. This constraint can also be implemented as a second-order cone constraint, if necessary. Note that, for the first step, the reachability constraint does not require linear approximations of $\sin\theta_0$ and $\cos\theta_0$, as the rotation of the stance foot is fixed.

F. Linear Rotation Approximation

To calculate s_j and c_j, a set of piecewise linear equations are introduced [1]. Let $S \in \{0,1\}^{L\times L}$ and $C \in \{0,1\}^{L\times L}$ be binary matrices, where L is the number of segments that compose the approximations. Then the constraints

$$S_{l,j} \Rightarrow \begin{cases} \phi_l \leq \theta_j \leq \phi_{l+1} \\ s_j = g_l\theta_j + h_l \end{cases}, \quad C_{l,j} \Rightarrow \begin{cases} \phi_l \leq \theta_j \leq \phi_{l+1} \\ c_j = g_l\theta_j + h_l \end{cases}, \quad (22)$$

are linear approximations of $\sin\theta$ and $\cos\theta$ in L segments, where g_l and h_l are the slope and intercept of segment l. We have found $L = 5$ to be a sufficient number of segments to approximate $\sin\theta$ and $\cos\theta$. The *implies* operator in Eq. (22) can be converted to linear constraints using the standard big-M formulation. By adding the additional constraints

$$\Sigma_{l=1}^{L} S_{l,j} = 1, \ \Sigma_{l=1}^{L} C_{l,j} = 1, \ \forall j = 1, \cdots, (m-1), \quad (23)$$

the selection of only one of the piecewise approximations in Eq. (22) is enforced. This formulation results in a mixed-integer quadratically constrained quadratic program (MIQCP) [1].

By using $m > 1$, the MPC can act as a local check on the feasibility of the footstep plan determined by the high level planner. Often, these plans do not include a dynamic model in order to increase computational efficiency

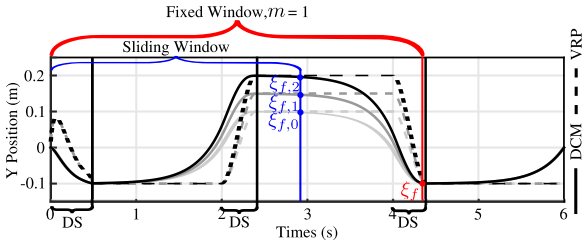

Fig. 4. DCM and VRP trajectories with footstep adjustment. The darker colored lines denote trajectories with a higher degree of step adjustment.

for online implementation. By allowing step position and rotation to be chosen by the dynamic planner, footstep plans with better dynamic performance are then found at execution.

G. Defining the Preview Window

Selecting the appropriate preview window size is critical for proper implementation when treating step location as a decision variable. Sliding preview windows of fixed size have been used [5, 11, 19]; however, when allowing step position to vary, this is not a viable option for the DCM, as the change in step position results in a change in the final desired value, $\boldsymbol{\xi}_f$, as shown in blue in Fig.4. Instead, the preview window can be defined to span to the end of the double support following the $m^{th}+1$ step, making $\boldsymbol{\xi}_f$ constant, shown in red in Fig.4.

V. Simulation Results

The MIQCP was solved using the commercial optimization package, Gurobi. Figure 5 shows the resulting DCM trajectories for a four step plan with a $2s$ step duration

TABLE I
DCM MPC Weights

Weight	D	F	Q	R	T	V	m
Plan	1e-4	1e6	2	5e-4	3.5	100	2
Simulation	1e-4	1e7	2	5e-4	3.5	2.5	2

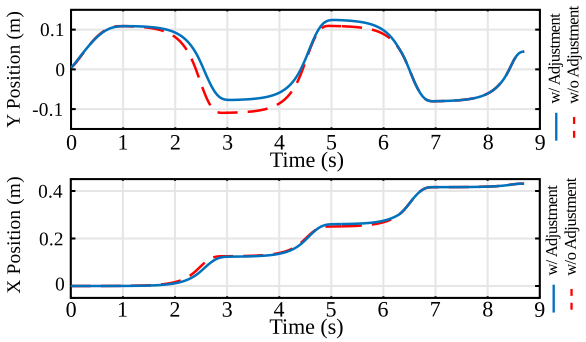

Fig. 5. DCM trajectories generated using MPC scheme, with and without allowing the step positions to vary.

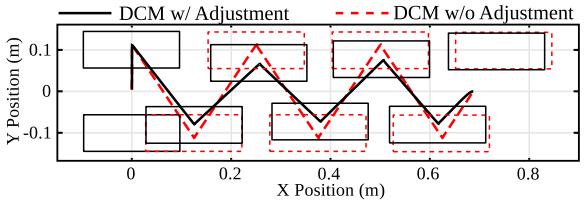

Fig. 6. Six step plan generated with low weight on step placement. The original step positions are shown as dashed red boxes.

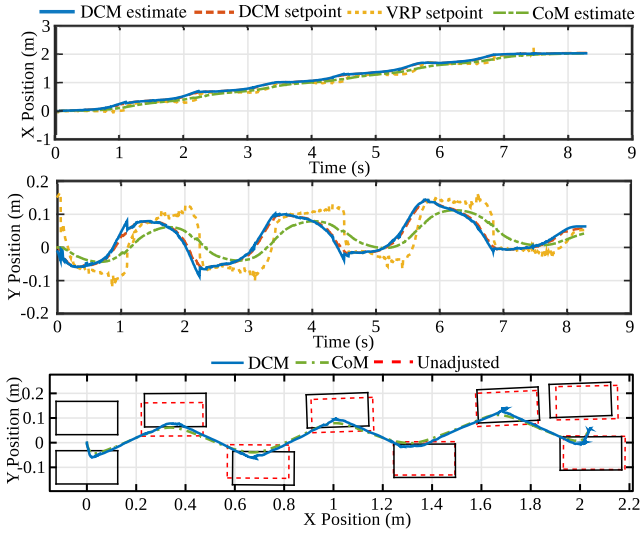

Fig. 7. Estimated and desired DCM trajectories while walking forward with step adjustment. Each step is $1s$ in duration with a double support duration of $0.3s$.

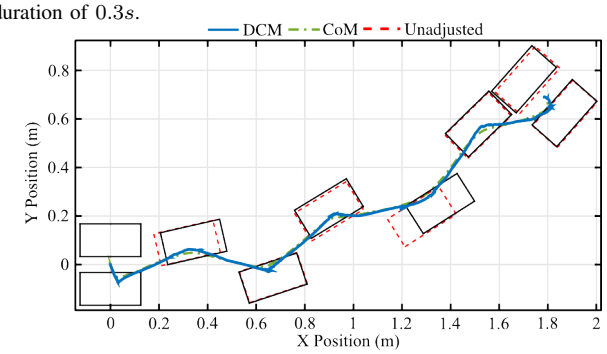

Fig. 8. Step adjustment while turning. Each step is $1s$ in duration with a double support duration of $0.3s$.

that turned $0.6rad$, where the first two steps were being optimized. The objective weights used are listed in Table I under row Plan, where $\mathbf{V}$ is a separate cost defined for rotation tracking. The reachability set was defined using x_{min} = 0.2 m, x_{max} = 0.4 m, y_{min} = 0.175 m, and y_{max} = 0.35 m. As can be seen, there was some degree of forward and lateral step adjustment to improve the DCM dynamics. Figure 6 shows trajectories generated for a six step plan using the same parameters used to generate the trajectories in Fig.5, but with $\mathbf{T}$ decreased to 0.75. In this case, all six steps were considered by the optimization, resulting in inward adjustment, as expected, to reduce lateral sway.

When implementing the MPC scheme in the motion framework, the desired momentum rate of change objective is achieved using a model-based whole-body controller presented in [14]. For real time implementation, $\mathbf{v}_{\dot{\xi}}$ is discretized at $\Delta t = 0.05s$, yielding an average solution time of $0.0721s$ when considering m=2 steps that have a $1.5s$ step duration. To account for this long solve time, the MPC solver is run on a separate thread, using the tracking control law from [11] to track the DCM trajectory between solutions. When the MPC solution is found, minimum jerk swing foot pose and torso orientation trajectories are also replanned to the new step position. The MPC is stopped for the last $0.05s$ of single support to prevent rapid step position changes before heel strike. Whole-body motions are executed using a 38-DoF model of ESCHER [23], simulated in Gazebo. ESCHER is a 77.5-kg torque-controlled humanoid developed for the DARPA Robotics Challenge.

Figure 7 shows the results of a six step plan executed by ESCHER, with a step length of $0.35m$, desired CoM height of $0.925m$, total step duration of $1s$ and a double support duration of $0.3s$. The reference CoP trajectories are designed to pass through $2cm$ on the inside of the feet, as this has been shown to increase the stability when walking [15]. The MPC weights selected for these simulations are listed in Table I under row Simulation. As seen in Fig.7, the robot was able to generate and track smooth DCM setpoints using the presented MPC scheme, resulting in slight adjustment to stabilize the rapid CoM motion. Figure 8 changes the step length to $0.3m$ and adds a total turning of $0.9rad$, resulting in step adjustment to improve and stabilize the DCM dynamics, producing smooth DCM setpoints. This demonstrates the ability for the MPC scheme to adjust the step positions from the nominal plan for improved dynamics and stabilization.

Figure 9 shows the resulting trajectories when a $200N$ lateral disturbance, equivalent to 26% of the weight of the robot, is applied to the torso for $0.1s$ midway through the third step. The plan consists of six steps with a total step duration of $1.5s$, double support duration of $0.45s$, and step length of $0.2m$. The disturbance resulted in a $9.4cm$ outward adjustment, with convergence back to nominal trajectories after one step. Figure 10 shows the resulting trajectories when a $175N$ lateral and $200N$ forward disturbance, equivalent to 35% of the weight of the robot, is applied to the torso for $0.1s$ midway through the third step of the same step plan. This disturbance resulted in a $6.8cm$ outward adjustment and $5.3cm$ forward adjustment, with an additional $5.1cm$ outward adjustment on the following step, resulting in stabilization of the CoM after two steps. The step adjustments in both Figs.9 and 10 allow the CoP to remain within the support

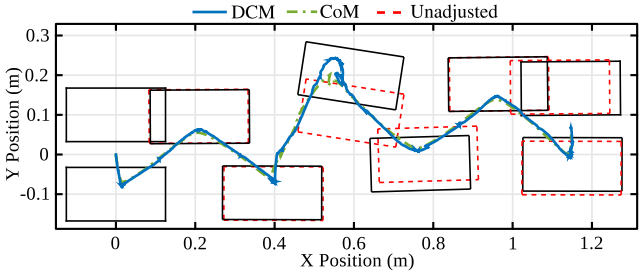

Fig. 9. Six step plan with a $1.5s$ step duration, $0.45s$ double support duration, and $200N$ lateral push on the third step.

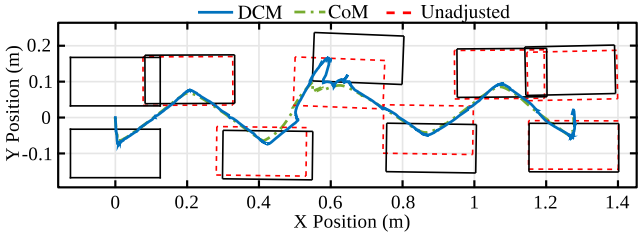

Fig. 10. Six step plan with a $1.5s$ step duration, $0.45s$ double support duration, $175N$ lateral and $200N$ forward push on the third step.

polygon, producing achievable ground reaction forces to stabilize the CoM, demonstrating the ability of the presented MPC scheme for stabilization of the CoM using the step positions as control inputs.

VI. Conclusion

This work presents a novel extension of previous MPC schemes using the time-varying DCM. Controlling only the unstable CoM dynamics has been shown to be very effective, and using the time-varying DCM further improves control of the CoM height compared to the time-invariant CP and DCM methods. The MPC scheme was further expanded to a mixed-integer formulation to allow for consideration of the step rotation as a control input. These additions greatly expand the versatility of MPC schemes. The performance of this approach was evaluated through simulations of the ESCHER humanoid with the demonstration of fast, stable walking motions over flat terrain, as well as adjusting the step position to reject large disturbances.

The proposed approach is currently being ported to the ESCHER hardware platform. The current formulation has the limitation of solve time too long for finding a solution at each time step. Additionally, the assumption of fixed step durations prevents early heel strike for recovery, which will be included as a decision variable in future work. The expansion of the proposed MPC scheme into a full footstep planner that considers the CoM dynamics is being explored.

Acknowledgments

This material is supported by ONR through grant N00014-15-1-2128 and by NSF through award 1525972. We would like to thank the team who contributed to the development of ESCHER. Special thanks to Michael Hopkins for his advice on implementation of the MPC problem.

References

[1] R. Deits and R. Tedrake, "Footstep planning on uneven terrain with mixed-integer convex optimization," in *Humanoid Robots (Humanoids), 14th IEEE-RAS International Conference on*, Nov 2014.

[2] J. Chestnutt, J. Kuffner, K. Nishiwaki, and S. Kagami, "Planning biped navigation strategies in complex environment," in *Humanoid Robots (Humanoids), 3rd IEEE-RAS International Conference on*, Oct 2003.

[3] A. Hornung, A. Dornbush, M. Likhachev, and M. Bennewitz, "Anytime search-based footstep planning with suboptimality bounds," in *Humanoid Robots (Humanoids), 2012 12th IEEE-RAS International Conference on*, Nov 2012, pp. 674–679.

[4] S. Kajita, F. Kanehiro, K. Kaneko, K. Yokoi, and H. Hirukawa, "The 3D linear inverted pendulum mode: a simple modeling for a biped walking pattern generation," in *Intelligent Robots and Systems (IROS), IEEE/RSJ International Conference on*, vol. 1, 2001, pp. 239–246.

[5] S. Kajita, F. Kanehiro, K. Kaneko, K. Fujiwara, K. Harada, K. Yokoi, and H. Hirukawa, "Biped walking pattern generation by using preview control of zero-moment point," in *Robotics and Automation (ICRA), IEEE International Conference on*, vol. 2, 2003, pp. 1620–1626.

[6] S. Kajita, M. Morisawa, K. Miura, S. Nakaoka, K. Harada, K. Kaneko, F. Kanehiro, and K. Yokoi, "Biped walking stabilization based on linear inverted pendulum tracking," in *Intelligent Robots and Systems (IROS), IEEE/RSJ International Conference on*, Oct 2010, pp. 4489–4496.

[7] T. Sugihara, "Standing stabilizability and stepping maneuver in planar bipedalism based on the best COM-ZMP regulator," in *Robotics and Automation (ICRA), IEEE International Conference on*, May 2009, pp. 1966–1971.

[8] P. Sardain and G. Bessonnet, "Forces acting on a biped robot. Center of Pressure-Zero Moment Point," *Systems, Man and Cybernetics, Part A: Systems and Humans, IEEE Transactions on*, vol. 34, no. 5, pp. 630–637, Sept 2004.

[9] J. Pratt, J. Carff, S. Drakunov, and A. Goswami, "Capture Point: A Step toward Humanoid Push Recovery," in *Humanoid Robots (Humanoids), 6th IEEE-RAS International Conference on*, Dec 2006, pp. 200–207.

[10] J. Englsberger, C. Ott, and A. Albu-Schaffer, "Three-dimensional bipedal walking control using Divergent Component of Motion," in *Intelligent Robots and Systems (IROS), IEEE/RSJ International Conference on*, Nov 2013, pp. 2600–2607.

[11] M. A. Hopkins, D. W. Hong, and A. Leonessa, "Humanoid locomotion on uneven terrain using the time-varying Divergent Component of Motion," in *Humanoid Robots (Humanoids), 14th IEEE-RAS International Conference on*, Nov 2014.

[12] M. Morisawa, S. Kajita, F. Kanehiro, K. Kaneko, K. Miura, and K. Yokoi, "Balance control based on Capture Point error compensation for biped walking on uneven terrain," in *Humanoid Robots (Humanoids), 12th IEEE-RAS International Conference on*, Nov 2012, pp. 734–740.

[13] J. Englsberger, T. Koolen, S. Betrand, J. Pratt, C. Ott, and A. Albu-Schaffer, "Trajectory generation for continuous leg forces during double support and heel-to-toe shift based on divergent component of motion," in *Intelligent Robots and Systems (IROS), IEEE/RSJ International Conference on*, Sept 2014.

[14] M. A. Hopkins, D. W. Hong, and A. Leonessa, "Compliant locomotion using whole-body control and Divergent Component of Motion tracking," in *Robotics and Automation (ICRA), IEEE International Conference on*, May 2015.

[15] M. A. Hopkins, R. J. Griffin, A. Leonessa, B. Y. Lattimer, and T. Furukawa, "Design of a compliant bipedal walking controller for the DARPA Robotics Challenge," in *Humanoid Robots (Humanoids), 2015 15th IEEE-RAS International Conference on*, 2015.

[16] P.-B. Wieber, "Trajectory free linear model predictive control for stable walking in the presence of strong perturbations," in *Humanoid Robots (Humanoids), 6th IEEE-RAS International Conference on*, Genova, Italy, Dec 2006, pp. 137–142.

[17] H. Diedam, D. Dimitrov, P. B. Wieber, K. Mombaur, and M. Diehl, "Online walking gait generation with adaptive foot positioning through linear model predictive control," in *Intelligent Robots and Systems (IROS), IEEE/RSJ International Conference on*, Sept 2008, pp. 1121–1126.

[18] A. Herdt, H. Diedam, P.-B. Wieber, D. Dimitrov, K. Mombaur, and M. Diehl, "Online walking motion generation with automatic footstep placement," *Advanced Robotics*, vol. 24, no. 5-6, pp. 719–737, 2010.

[19] M. Krause, J. Englsberger, P.-B. Wieber, and C. Ott, "Stabilization of the capture point dynamics for bipedal walking based on model predictive control," in *IFAC Symposium on Robot Control (SYROCO)*, vol. 10, no. 1, 2012, pp. 165–171.

[20] J. Park and Y. Youm, "General ZMP preview control for bipedal walking," in *Robotics and Automation, 2007 IEEE International Conference on*, April 2007, pp. 2682–2687.

[21] J. Mayr, H. Gattringer, and H. Bremer, "Online walking gait generation with predefined variable height of the center of mass," in *Intelligent Robotics and Applications*, ser. Lecture Notes in Computer Science, S. Jeschke, H. Liu, and D. Schilberg, Eds. Springer Berlin Heidelberg, 2011, vol. 7102, pp. 569–578.

[22] S. Kuindersma, F. Permenter, and R. Tedrake, "An efficiently solvable quadratic program for stabilizing dynamic locomotion," in *Robotics and Automation (ICRA), IEEE International Conference on*, May 2014.

[23] C. Knabe, J. Seminatore, J. Webb, M. Hopkins, A. Leonessa, B. Y. Lattimer, and T. Furukawa, "Design of a series elastic humanoid for the DARPA Robotics Challenge," in *Humanoid Robots (Humanoids), 2015 15th IEEE-RAS International Conference on*, 2015.